Asian Journal of Chemistry; Vol. 35, No. 5 (2023), 1250-1256

ASIAN JOURNAL OF CHEMISTRY

https://doi.org/10.14233/ajchem.2023.27654

Synthesis and Characterization of Pure and Cu-doped NiO Thin Films for Detection of Ethanol

K. RAJESH[1,*], NAGARAJU POTHUKANURI[2] and M.V. RAMANA REDDY[1,3]

[1]Thin Films and Nanomaterials Research Laboratory, Department of Physics, Osmania University, Hyderabad-500007, India
[2]Department of Physics, Sreenidhi University, Ghatkesar, Hyderabad-501301, India
[3]Department of Physics, JNTUH College of Engineering Science and Technology, Hyderabad-500085, India

*Corresponding author: E-mail: rajeshbhu1234@gmail.com

Received: 17 February 2023; *Accepted*: 18 April 2023; *Published online*: 28 April 2023; AJC-21236

Herein, a highly sensitive, selective and stable ethanol sensor based on nanostructured Cu doped NiO thin films is reported. Pure and Cu doped NiO thin films were prepared using spray pyrolysis technique with different copper concentrations. The XRD, Raman, SEM, XPS and TEM were used to investigate the structural, morphological and compositional properties of deposited films. The XRD studies confirmed that deposited films exhibit cubic structure with polycrystalline nature. Raman spectroscopy of the deposited NiO based thin film reveals as single-phonon first-order longitudinal-optical LO mode and double-phonon second-order longitudinal-optical mode 2LO. Scanning electron microscopy (SEM) has demonstrated a significant variation in the morphology of the coated films. X-ray photoelectron spectroscopy (XPS) results revealed that successful doping of copper in NiO matrix, whereas TEM investigations revealed a nanometric crystal size in Cu doped NiO. Gas sensing performance of the deposited thin films was measured using static distribution technique towards 50 ppm ethanol gas at room temperature. Cu doped NiO thin film (4 wt.%) has shown improved sensing features towards 50 ppm of ethanol with good selective, sensitive and stable features with quick response and recovery characteristics.

Keywords: NiO thin-film, Spray pyrolysis, Ethanol sensor.

INTRODUCTION

In recent past, a great deal of attention has been focused by the researchers across the world for reliable gas sensors due to their various applications such as industrial control systems, house-hold safety and security, fuel emission and environmental pollution monitoring [1-3]. The metal oxide based semiconductor gas sensors have grabbed huge attention by the researchers across the world due to their cost-effective, portability, quick response and long term durability [4-7]. The gas sensing properties are closely connected with the morphological, surface properties and chemical composition of the metal oxides. Among all metal oxides, NiO is a wide bandgap semiconductor with the most prominent cubic structure [8]. It has a wide range of applications, including electrochromic display devices, solar cells, smart windows, optoelectronic devices, cathode material for battery applications, solid oxide fuel cells, antiferromagnetic material and active material in chemical gas sensors [9,10], heterojunction solar cells [11] and active layer materials for gas sensors [12] due to low cost raw materials and excellent chemical and thermal stability.

Jang *et al.* [13] with RF magnetron sputtering synthesized lithium doped NiO films with concentration variation from 0 to 16 wt.% on glass substrates. The outcome of this study demonstrated that the electrical resistivity was increased due to the crystal imperfections on the surface of thin film. However, some lithium ions isolated on the film surface and bulges. Lou *et al.* [14] reported the preparation and characterization of Al doped boron substituted nickel oxide thin films using sol-gel technique. The results demonstrated that Al doping might hamper the formation of crystalline thin films, which have shown good electrochromic and electrochemical characteristics, in comparison with pure NiO thin film samples. Studies on Fe doped nickel oxide films deposited using spray pyrolysis Technique has been investigated by Godbole *et al.* [15]. They reported that with an increase in the thickness of the film, the density of states at the Fermi-energy level enhances. The transmittance of the films was found to enhance with the deposition

temperature. The impact of Cu doping on nickel oxide films deposited with electrochemical deposition method was reported by Zhao *et al.* [16]. The authors studied that the decrease in transmittance of the films upon doping of Cu in nickel oxide thin films with excellent electrochromic behaviour. It is also observed that chemical composition, surface morphology, uniformity, conductivity and absorbance could depend on the nature of doping element and process [17]. Energy band gap can be varied drastically with the doping of monovalent impurities such as lithium, indium, sodium and copper. Also the electrical resistivity of NiO films may be reduced with doping. Hence, Cu doped NiO thin films play a vital role in gas sensor applications [18].

Ethanol (C_2H_5OH) is widely utilized as a solvent in many industries such as chemical, food, alcoholic beverages and biomedical industries. It is also a hypnotic solvent with toxic in nature, colourless and inflammable [19]. High exposure or utilization of ethanol, especially by smokers leads to lung cancer, liver deterioration and breast cancer among the women. Industrial employers where ethanol can release frequently may increase the possibility of affecting the respiratory system and digestive track cancer. Hence, an ethanol sensor which is operating under ambient conditions will be very essential for public transportation systems [20]. In this study, a low-cost NiO-based chemiresistive ethanol sensor is developed which can detect low levels of analyte gas at ambient temperature.

EXPERIMENTAL

The required materials for the synthesis of thin films were nickel(II) acetate tetrahydrate [$Ni(CH_3COO)_2{\cdot}4H_2O$] analytical grade (Sigma-Aldrich, India) and copper(II) acetate hydrate ($Cu(CH_3COO)_2{\cdot}H_2O$] analytical grade (Sigma Aldrich, India) salts were utilized with a purity larger than ≥ 99%. The solvent employed throughout the experiment was double-deionized water. The glass slides (Blue Star, India) having dimensions of 7.5 cm × 2.5 cm × 0.135 cm were used as substrates.

Synthesis and characterizations of pure and Cu doped NiO thin films: Nickel(II) acetate tetrahydrate was added to 20 mL double deionized water and stirred for 30 min. Citric acid has been added drop wise to the above salt solution to make it transparent and clear. Copper(II) acetate hydrate was added to 20 mL of double deionized water separately and stirred for 30 min. Then, it was mixed with the nickel acetate solution dropwise subsequently stirred for few minutes. Obtained solution was loaded to spray dispenser of fully automated spray pyrolysis system (Holmarc, India) connected with a computer and sprayed for 12 min on preheated clean glass slides.

The prepared film's thickness was determined using weight difference method with a sensitive microbalance. The deposition parameters are shown in Table-1. The structural properties of the prepared films were investigated with the X-ray diffraction technique with Bruker D8 advance system utilizing CuK_α as energy source. Morphological analysis was done with FESEM-FEI NoVaNanoSEM 450 instrument. Structural distinctions of deposited samples were studied using Ar laser source having wavelength of 488 nm switched to Labram-HR800 Raman spectrometer with the Raman backscattering geometry under ambient conditions. Transmission electron microscope (model TECNAI 20G2) working at 200 kV voltage was used to study nanostructured nature and grain distribution. Homemade gas-sensing system in static mode which was interfaced to a computerized Keithley electrometer (6517B, USA) was used for gas sensing measurements.

TABLE-1
DEPOSITION PARAMETERS

Parameters	Specification
Precursor	Nickel(II) acetate tetrahydrate and copper(II) acetate hydrate
Solvent	Deionized water
Concentration of the precursor	0.1 M
Doping concentration	2, 4, 6 wt.% of copper
Substrate	Glass
Deposition temperature	400 °C
Nozzle to substrate distance	20 cm
Deposition time	12 min
Carrier gas	Air
Carrier gas pressure	1 bar
Flow rate	1 mL/min

RESULTS AND DISCUSSION

XRD: The XRD patterns of pure and copper doped nickel oxide thin films with different doping concentration are shown in Fig. 1. Four diffraction reflections located at Bragg's angles of 37.2º, 43.2º, 62.8º and 75.3º were observed. According to JCPDS data card No. 78-0423, all these peaks of NiO films are related with the cubic structure without any impurity phase. Shift towards higher angles in diffraction peaks observed with doping due to mismatch of Cu ions (0.82 Å) and Ni ions (0.78 Å) radius. Compared to pure NiO more broad peaks are observed for Cu doped NiO films [21,22]. The crystallite size (D) was determined for (200) plane using the Scherrer's formula [23]. The Cu-Cu ion interactions may be the reason for increased crystallite size for doped samples [24].

$$\text{Crystallite size (D)} = \frac{0.9\lambda}{\beta\cos\theta} \quad (1)$$

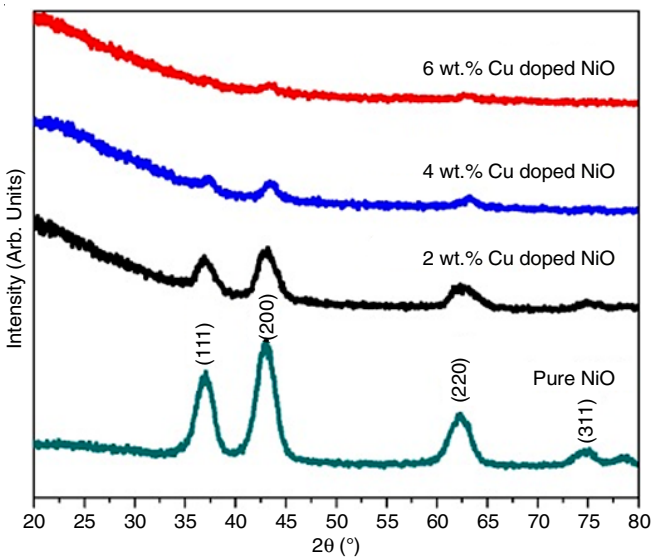

Fig. 1. XRD pattern of pure and Cu doped NiO thin film

where λ, β and θ denotes X-ray wavelength, FWHM and Bragg's angle, respectively.

The obtained XRD data has been used to calculate the structural properties including the interplanar distance (d), lattice constant (a), volume of unit cell (V), crystallite dimension (D), strain (ε), dislocation density (δ) and count of crystallites per unit area (N). Interplanar distance (d) can be calculated using Bragg's formula [25,26]. The obtained structural parameters are tabulated in Table-2.

$$\text{Dislocation density } (\delta) = \frac{1}{(\text{Crystallite size})^2} \quad (2)$$

$$\text{Strain } (\varepsilon) = \frac{\beta \cos\theta}{4} \quad (3)$$

$$\text{Crystallites occupied per unit area (M)} = \frac{\text{Thickness of the film}}{(\text{Crystallite size})^3} \quad (4)$$

$$\text{Inter planar spacing (d)} = \frac{\lambda}{2\sin\theta} \quad (5)$$

$$\text{Lattice constant (a)} = d \times \sqrt{h^2 + k^2 + l^2} \quad (6)$$

$$\text{Volume of unit cell} = a^3 \quad (7)$$

SEM studies: Fig. 2 clearly shows the effect of doping on the morphological studies. Pure nickel oxide thin films have shown flake like morphology whereas NiO thin films of 2 wt.% Cu doped randomly oriented morphology was observed. NiO thin films of 4 wt.% Cu doped, spherical shaped particles with uniform size were distributed on the surface. It can be inferred that this sample can be suitable for the gas sensing applications.

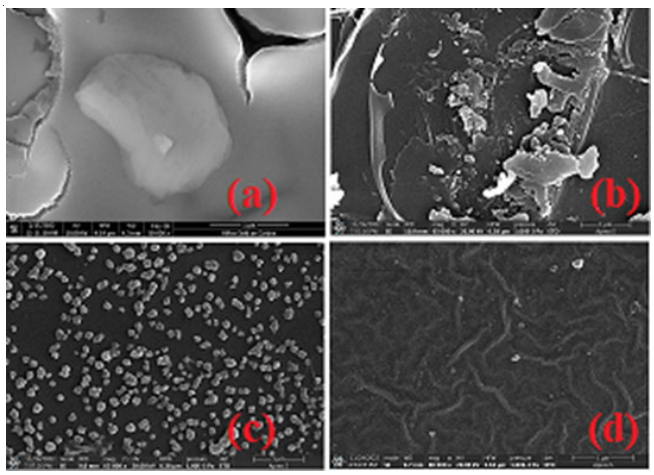

Fig. 2. SEM images of (a) pure (b) 2 wt.% (c) 4 wt.% d) 6 wt.% doped Cu: NiO thin films

Raman studies: Raman spectrum of pure and doped films synthesized with various Cu doping concentrations is depicted in Fig. 3. Two important major peaks are appeared in pure NiO thin films at 550 and 1090 cm^{-1} which are related as single-phonon first-order longitudinal-optical LO mode and double-phonon second-order longitudinal-optical mode 2LO respectively, which confirms the NiO formation [27] for Cu doped NiO films, a shift of peak position in one-phonon first-order longitudinal-optical LO mode was observed and can be associated with the structural defects and vacancies created during the deposition process in the nanostructured material. A small shift in the 2LO mode was observed, which can be due to an enhancement in the crystallite size.

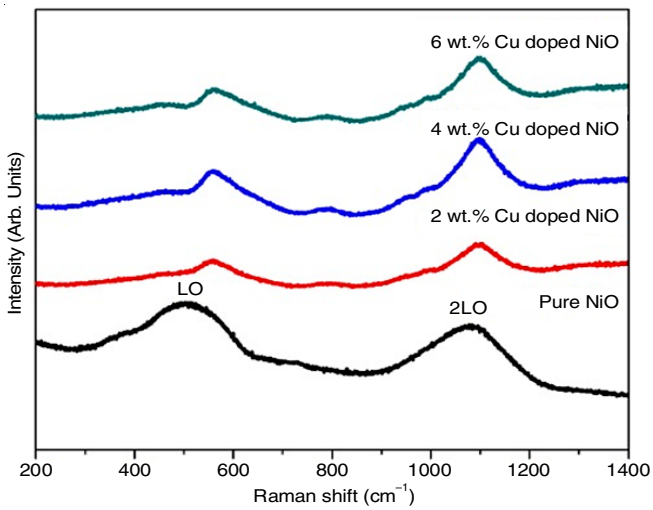

Fig. 3. Raman spectra of pure and Cu doped NiO thin film

XPS measurements: The chemical composition on the surface and valance electronic states of the NiO thin film with 4 wt.% Cu doped were measured with XPS technique. A full scan of NiO thin film with 4 wt.% Cu doped is shown in Fig. 4. Without any foreign elements present, an XPS scan confirmed the presence of nickel, copper and oxygen, indicating that grown film had the proper composition during the spray process. The peaks at binding energies of 854 eV (Ni $2p_{3/2}$) and 873 eV (Ni $2p_{1/2}$) assigned to Ni^{2+} suggest the presence of NiO. The Cu2p signals, which correspond to $Cu2p_{3/2}$ and $Cu2p_{1/2}$, were observed in the spectrum at positions 932.5 and 952.6 eV. Two spectral lines have been obtained from the XPS O 1s spectrum, one of which relates to the metal oxide lattice site and the other peak being connected to adsorbed oxygen. While O1s assigned peak was observed at 529.6 eV and Cu 2p at 933.07 eV. These values shown to be consistent with previous investigations [28,29].

TABLE-2
STRUCTURAL PARAMETERS OF PURE AND Cu DOPED NiO THIN FILM

Sample	Crystallite size (D) nm	Dislocation density × 10^{16} (lines/m^2)	Strain	Number of crystallites per unit area × 10^{18}	Thickness (nm)	Interplanar spacing (Å)	Lattice constant (Å)	Volume of unit cell × 10^{-29} (m^3)
Pure NiO	4.20	5.64	0.008300	21.21	376	2.102	4.204	7.43161
2 wt.% Cu doped NiO	4.31	5.37	0.008170	9.83	183	2.098	4.196	7.38790
4 wt.% Cu doped NiO	6.77	2.18	0.005206	1.39	64	2.084	4.167	7.24045
6 wt.% Cu doped NiO	8.69	1.32	0.004055	1.27	96	2.088	4.176	7.28391

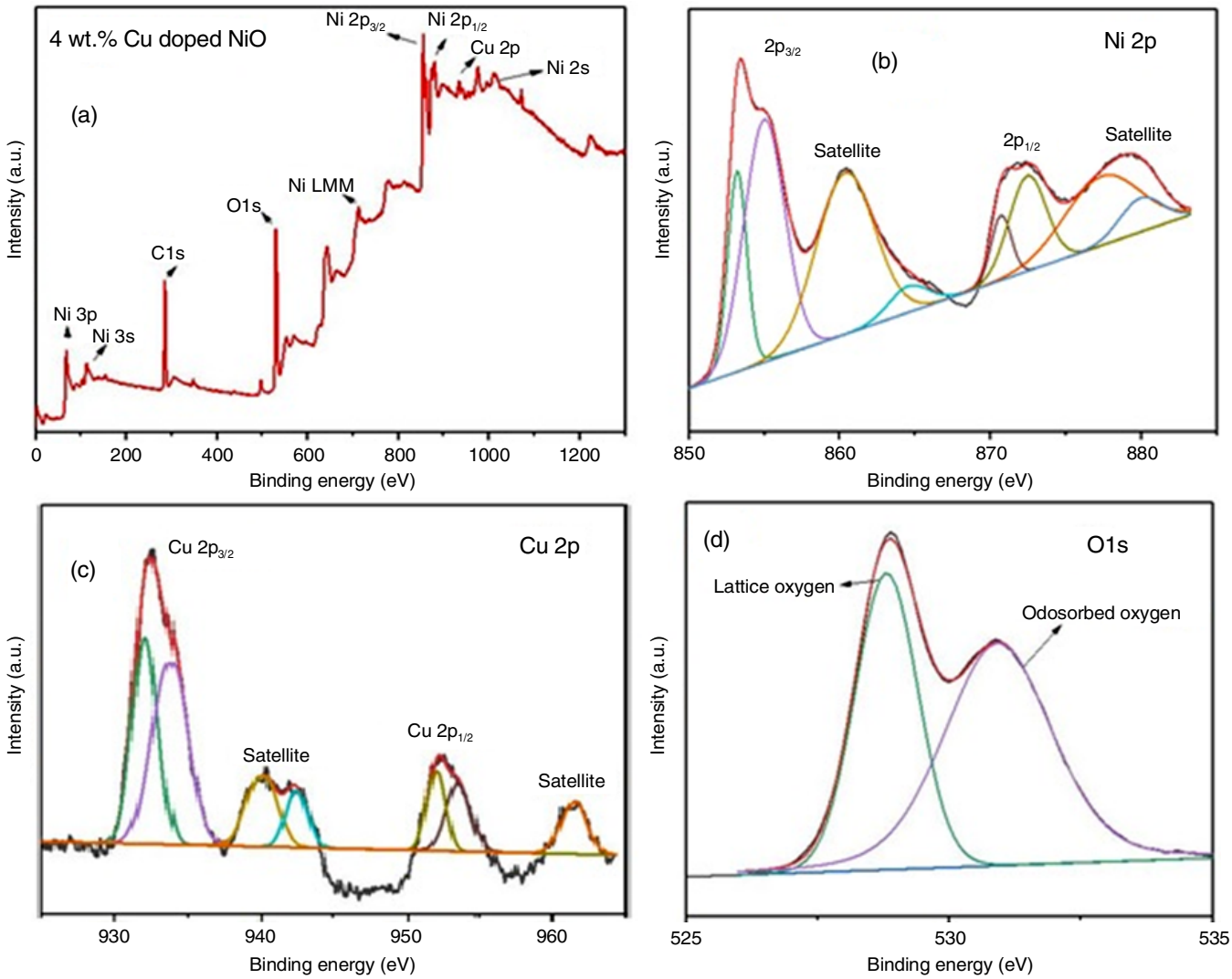

Fig. 4. (a) XPS full scan of 4 wt.% Cu doped NiO thin film. High-resolution spectra of (b) Ni 2p, (c) Cu 2p and (d) O1s

TEM studies: Fig. 5 shows HRTEM images of NiO thin film of 4 wt.% copper with crystallinity in the nanostructured range which is consistent with the XRD pattern. Fig. 6 depicts SAED pattern with the set of diffraction rings confirms the polycrystalline nature of deposited film.

Gas sensing properties: Response is an important parameter of a chemiresistive based gas sensor. In reducing/oxidizing gas environment, a chemiresistive sensor, changes its electrical resistance. The response of chemiresistive sensor might be studied considering the changes in resistance under test gas environment. Sensor element response mainly depends on the working temperature, surface roughness, films' thickness, deposition method of the thin film, surface to volume ratio, porosity, space between the grains, adsorption by oxygen molecules at the film surface and elements present in the material [29-33]. The sensing layer response was determined using eqn. 10 [34]:

$$\text{Response of the sensor layer} = \frac{R_a}{R_g} \qquad (10)$$

where R_a and R_g denote sensor layer resistance under dry air and reducing gas environment, respectively.

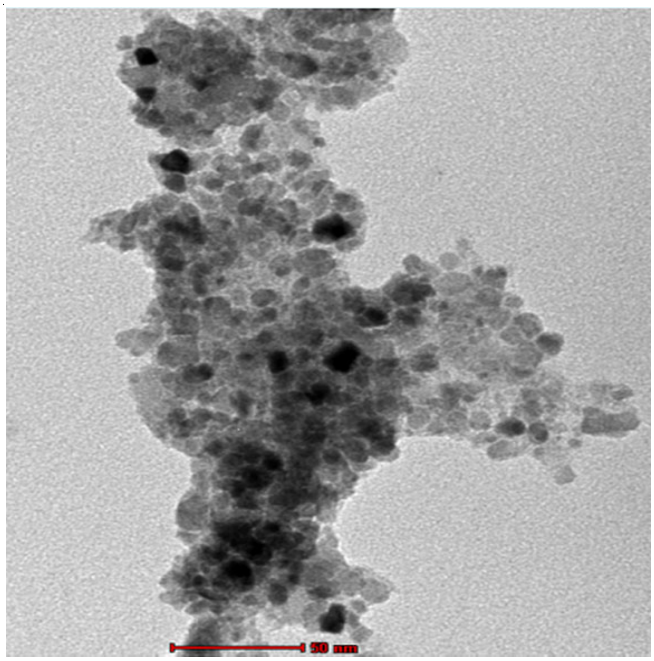

Fig. 5. TEM image of 4 wt.% Cu doped NiO thin film

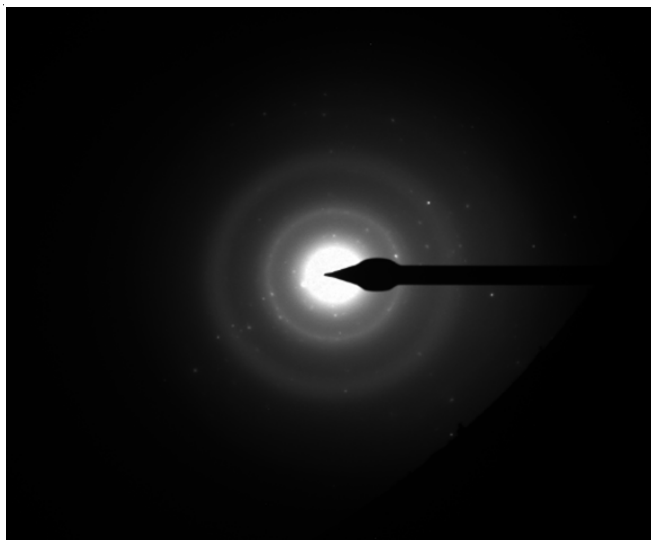

Fig. 6. SAED pattern of 4 wt.% Cu doped NiO thin film

As one of the most challenges of the semiconductor gas sensors is selectivity. The proposed sensors have been investigated in the presence of various vapours namely benzene, acetone, methanol, isopropanol, 2-methoxy ethanol, *n*-butanol and ethanol of 50 ppm, respectively using liquid distribution technique. At room temperature, the trend shows that the gas response towards 50 ppm of ethanol is more selective than other gases (Fig. 7). As a result, ethanol is being studied further.

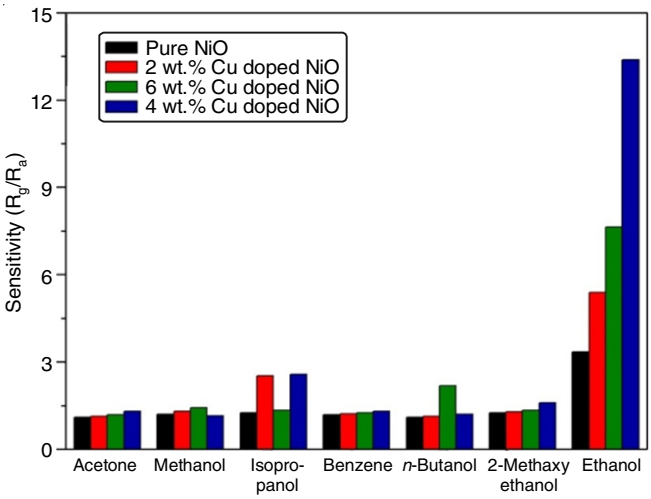

Fig. 7. Selectivity of Cu doped NiO thin film

Stability and repeatability are most important parameters for gas sensors. Figs. 8 and 9 show the stability and repeatability of 4 wt.% Cu doped NiO thin films towards 50 ppm ethanol at ambient temperature. Repeatability was checked for continuous four cycles whereas stability was checked over a period of 30 days which shown a negligible variation.

Fig. 10 depicts a 50 ppm ethanol transient response at room temperature. According to the study's findings, 4 wt.% Cu doped NiO thin film exhibits traditional p-type behaviour showing low resistance under dry air and the sensor's resistance rises under reducing gas (ethanol). Sensor element has a response time of 28 s and recovery time of 21 s.

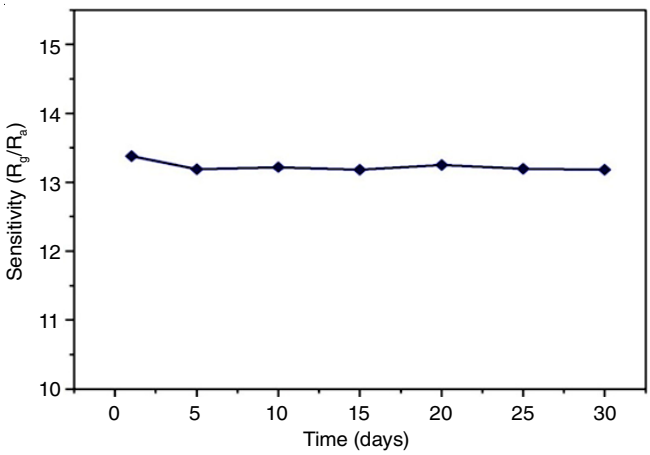

Fig. 8. Stability of 4 wt.% Cu doped NiO thin film towards ethanol

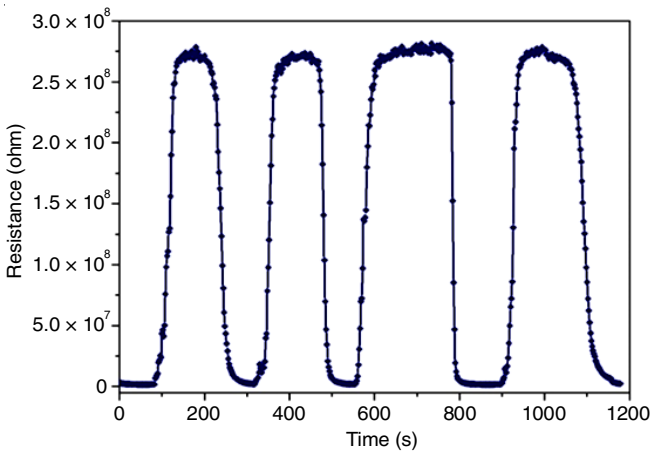

Fig. 9. Repeatability of 4wt.% Cu doped NiO thin film towards ethanol

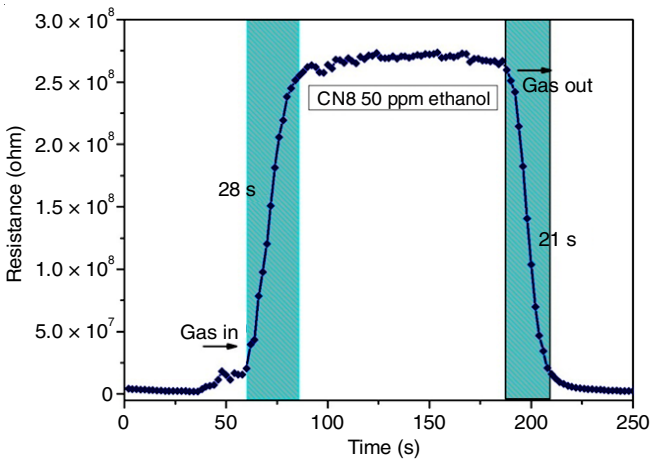

Fig. 10. Transient response curve of 4 wt.% Cu doped NiO thin film towards ethanol

Comparative studies: Table-3 summarizes an overview of the ethanol-sensing features of different several metal oxides found in the literature as well as the current investigation. The data clearly shows that the proposed Cu-doped NiO thin films towards the detection of ethanol gas exhibit quick response at low temparature as compared to the majority of the reported sensors.

TABLE-3
COMPARISON OF THE ETHANOL-SENSING CHARACTERISTICS OF VARIOUS METAL OXIDES WITH CURRENT WORK

Gas sensing material	Conc. (ppm)	Temp. (°C)	Response/ Recovery time	Ref.
NiO	5	350	80 s/2 min	[35]
NiO	5	350	167 s/99 s	[36]
NiO/SnO_2	1000	250	15 s/100 s	[37]
Fe-ZnO	100	320	39 s/29 s	[38]
ZnO-In_2O_3	50	240	35 s/46 s	[39]
Ag@SnO_2	200	27	34 s/68 s	[40]
Ag@TiO_2	5	27	52 s/63 s	[41]
Ga-NiO	50	250	8 s/13 s	[42]
Al-NiO	100	228	73 s/76 s	[43]
Sc/Li-NiO	100	200	86 s/31 s	[44]
Fe-NiO	50	240	7 s/8 s	[45]
Mg-NiO	100	325	13 s/19 s	[46]
Cu-NiO	50	27	28 s/21 s	Present work

Conclusion

Pure and Cu doped NiO films deposited by chemical spray pyrolysis method by varying doping concentration on preheated glass substrates. XRD investigations disclosed that synthesized films have exhibited polycrystalline behaviour with the cubic structure. Crystallite size is calculated with Scherrer equation and it is enhanced with doping concentration. Pure nickel oxide thin films have shown flake like morphology whereas thin films of 2 wt.% of Cu doped randomly oriented morphology was observed. 4 wt.% of Cu doped NiO film shown spherical shaped particles with uniform grain size were distributed on the surface which is shown high response against 50 ppm of ethanol under ambient conditions. This improvement in sensing characteristic is owing to sensor element properties like micro-structural, topographical features with high surface to volume ratio. Among all the films, the 4 wt.% Cu doped NiO sensor has a quick detection rate with high stability and repeatability can be transferred to fabricate an ethanol sensor for real time applications.

ACKNOWLEDGEMENTS

The authors thank The Head, Department of Physics, Osmania University, Hyderabad, India for providing necessary research facilities to carry out the work. One of the authors, (M.V.R.R) thank Prof.K.N. Reddy, Vice-Chancellor JNTU Hyderabad, India for his support and constant encouragement. Thanks are also due to Dr. V. Raghavendra Reddy, Scientist H and Dr. Vasanth Sathe, Scientist H, UGC-DAE-CSR, Indore, India for providing the XRD and Raman analysis, respectively.

CONFLICT OF INTEREST

The authors declare that there is no conflict of interests regarding the publication of this article.

REFERENCES

1. S.J. Mezher, M.O. Dawood, O.M. Abdulmunem and M.K. Mejbel, *Vacuum*, **172**, 109074 (2020); https://doi.org/10.1016/j.vacuum.2019.109074
2. A.M. Reddy, A.S. Reddy and P.S. Reddy, *Mater. Res.*, **678**, 361 (2013); https://doi.org/10.4028/www.scientific.net/AMR.678.361
3. S.J. Mezher, M.O. Dawood, A.A. Beddai and M.K. Mejbel, *Mater. Technol.*, **35**, 60 (2019); https://doi.org/10.1080/10667857.2019.1653595
4. A. Rydosz, A. Brudnik and K. Staszek, *Materials*, **12**, 877 (2019); https://doi.org/10.3390/ma12060877
5. M.A.M. Hassan, A.A. Hateef, A.M.A. Majeed, A.J.M. Al-Jabiry, S. Jameel and H.A.R.A. Hussian, *Appl. Nanosci.*, **4**, 927 (2014); https://doi.org/10.1007/s13204-013-0270-5
6. M.A.M. Hassan, A.F. Saleh and S.J. Mezher, *Appl. Nanosci.*, **4**, 695 (2014); https://doi.org/10.1007/s13204-013-0246-5
7. M.M. Kareem, S.J. Mezher and A.A. Beddai, *J. Non-Oxide Glasses*, **11**, 27 (2019).
8. K.K. Purushothaman and G. Muralidharan, *Sol. Energy Mater. Sol. Cells*, **93**, 1195 (2009); https://doi.org/10.1016/j.solmat.2008.12.029
9. Y. Makimura, A. Rougier and J.M. Tarascon, *Appl. Surf. Sci.*, **252**, 4593 (2006); https://doi.org/10.1016/j.apsusc.2005.07.086
10. M. Kitao, K. Izawa, K. Urabe, T. Komatsu, S. Kuwano and S. Yamada, *Jpn. J. Appl. Phys.*, **33(12R)**, 6656 (1994); https://doi.org/10.1143/JJAP.33.6656
11. J. Bandara, C.M. Divarathne and S.D. Nanayakkara, *Sol. Energy Mater. Sol. Cells*, **81**, 429 (2004); https://doi.org/10.1016/j.solmat.2003.11.027
12. K. Ganga Reddy, P. Nagaraju, G.L.N. Reddy, P. Ghosal and M.V.R. Reddy, *Sens. Actuators A Phys.*, **346**, 113876 (2022); https://doi.org/10.1016/j.sna.2022.113876
13. W.-L. Jang, Y.-M. Lu, W.-S. Hwang and W.-C. Chen, *J. Eur. Ceram. Soc.*, **30**, 503 (2010). https://doi.org/10.1016/j.jeurceramsoc.2009.05.041
14. X. Lou, X. Zhao and X. He, *Solar Energy*, **83**, 2103 (2009); https://doi.org/10.1016/j.solener.2009.06.020
15. B. Godbole, N. Badera, S. Shrivastava, D. Jain and V. Ganesan, *Surf. Rev. Lett.*, **14**, 1113 (2007); https://doi.org/10.1142/S0218625X07010688
16. L. Zhao, G. Su, W. Liu, L. Cao, J. Wang, Z. Dong and M. Song, *Appl. Surf. Sci.*, **257**, 3974 (2011); https://doi.org/10.1016/j.apsusc.2010.11.160
17. A.D. Shweta Moghe, *Renew. Energy*, **29**, 647 (2013).
18. I. Manouchehri, D. Mehrparvar, R. Moradian, K. Gholami and T. Osati, *Optik*, **127**, 8124 (2016); https://doi.org/10.1016/j.ijleo.2016.06.005
19. M. Mohammed, A.A. Wiles, M. Belsley, S.S.M. Fernandes, M. Cariello, V.M. Rotello, M.M.M. Raposo and G. Cooke, *RSC Adv.*, **7**, 24462 (2017); https://doi.org/10.1039/C7RA03400H
20. D. Zhu, Y. Fu, W. Zang, Y. Zhao, L. Xing and X. Xue, *Mater. Lett.*, **166**, 288 (2016); https://doi.org/10.1016/j.matlet.2015.12.106
21. Q. Hu, W. Li, D.I. Abouelamaiem, C. Xu, H. Jiang, W. Han and G. He, *RSC Adv.*, **9**, 20963 (2019); https://doi.org/10.1039/C9RA03780B
22. M.A. Hefnawy, S.A. Fadlallah, R.M. El-Sherif and S.S. Medany, *J. Alloys Compd.*, **896**, 162857 (2022); https://doi.org/10.1016/j.jallcom.2021.162857
23. S.G. Dasari, P. Nagaraju, V. Yelsani and M.V. Ramana Reddy, *J. Mater. Sci. Mater. Electron.*, **33**, 23447 (2022); https://doi.org/10.1007/s10854-022-09106-8
24. L. Zhao, G. Su, W. Liu, L. Cao, J. Wang, Z. Dong and M. Song, *Appl. Surf. Sci.*, **257**, 3974 (2011); https://doi.org/10.1016/j.apsusc.2010.11.160
25. S. Mani Menaka, G. Umadevi and M. Manickam, *Mater. Chem. Phys.*, **191**, 181 (2017); https://doi.org/10.1016/j.matchemphys.2017.01.048
26. D.S. Gavaskar, P. Nagaraju and M.V.R. Reddy, *Micropor. Mesopor. Mater.*, **345**, 112247 (2022); https://doi.org/10.1016/j.micromeso.2022.112247
27. G. Anandha Babu, G. Ravi, T. Mahalingam, M. Kumaresavanji and Y. Hayakawa, *Dalton Trans.*, **44**, 4485 (2015); https://doi.org/10.1039/C4DT03483J

28. A.M. Soleimanpour, A.H. Jayatissa and G. Sumanasekera, *Appl. Surf. Sci.*, **276**, 291 (2013); https://doi.org/10.1016/j.apsusc.2013.03.085
29. Q. Hu, W. Li, D.I. Abouelamaiem, C. Xu, H. Jiang, W. Han and G. He, *RSC Adv.*, **9**, 20963 (2019); https://doi.org/10.1039/C9RA03780B
30. N. Brilis, C. Foukaraki, E. Bourithis, D. Tsamakis, A. Giannoudakos, M. Kompitsas, T. Xenidou and A. Boudouvis, *Thin Solid Films*, **515**, 8484 (2007); https://doi.org/10.1016/j.tsf.2007.03.147
31. C.S. Rout, M. Hegde, A. Govindaraj and C.N.R. Rao, *Nanotechnology*, **18**, 205504 (2007); https://doi.org/10.1088/0957-4484/18/20/205504
32. U. Cindemir, Z. Topalian, C.G. Granqvist, L. Österlund and G.A. Niklasson, *Mater. Chem. Phys.*, **227**, 98 (2019); https://doi.org/10.1016/j.matchemphys.2019.01.058
33. C. Wang, T. Wang, B. Wang, X. Zhou, X. Cheng, P. Sun, J. Zheng and G. Lu, *Sci. Rep.*, **6**, 26432 (2016); https://doi.org/10.1038/srep26432
34. M. Tiemann, *Chem. Eur. J.*, **13**, 8376 (2007); https://doi.org/10.1002/chem.200700927
35. S.K. Ayyala and J.A. Covington, *Chemosensors*, **9**, 247 (2021); https://doi.org/10.3390/chemosensors9090247
36. I. Hotovy, L. Spiess, M. Predanocy, V. Rehacek and J. Racko, Vacuum, **107**, 129 (2014); https://doi.org/10.1016/j.vacuum.2014.04.012
37. J. Fang, Y. Zhu, D. Wu, C. Zhang, S. Xu, D. Xiong, P. Yang, L. Wang and P.K. Chu, *Sens. Actuators B Chem.*, **252**, 1163 (2017); https://doi.org/10.1016/j.snb.2017.07.013
38. Y. Shen, Q. Li, T. Li, M. Cao, F. Gu, L. Wang and D. Zhu, *J. Mater. Sci. Mater. Electron.*, **31**, 3074 (2020); https://doi.org/10.1007/s10854-019-02852-2
39. K. Zhang, S. Qin, P. Tang, Y. Feng and D. Li, *J. Hazard. Mater.*, **391**, 122191 (2020); https://doi.org/10.1016/j.jhazmat.2020.122191
40. R.-J. Wu, D.-J. Lin, M.-R. Yu, M.H. Chen and H.-F. Lai, *Sens. Actuators B Chem.*, **178**, 185 (2013); https://doi.org/10.1016/j.snb.2012.12.052
41. Z. Zhu, C.-T. Kao and R.-J. Wu, *Appl. Surf. Sci.*, **320**, 348 (2014); https://doi.org/10.1016/j.apsusc.2014.09.108
42. S. Shailja, K.J. Singh and R.C. Singh, *J. Mater. Sci. Mater. Electron.*, **32**, 11274 (2021); https://doi.org/10.1007/s10854-021-05796-8
43. M. ul Haq, Z. Zhang, Z. Wen, S. Khan, S. ud Din, N. Rahman and L. Zhu, *J. Mater. Sci. Mater. Electron.*, **30**, 7121 (2019); https://doi.org/10.1007/s10854-019-01030-8
44. J. Chang, M. Horprathum, D. Wang, G. Meng, Z. Deng, B. Tong, P. Kidkhunthod, T. Dai, M. Li, H. Liu, W. Tong, S. Wang and X. Fang, *Sens. Actuators B Chem.*, **326**, 128834 (2021); https://doi.org/10.1016/j.snb.2020.128834
45. X. Sun, X. Hu, Y. Wang, R. Xiong, X. Li, J. Liu, H. Ji, X. Li, S. Cai and C. Zheng, *J. Phys. Chem. C*, **119**, 3228 (2015); https://doi.org/10.1021/jp5124585
46. Y. Zhao, J. Yan, Y. Huang, J. Lian, J. Qiu, J. Bao, M. Cheng, H. Xu, H. Li and K. Chen, *J. Mater. Sci. Mater. Electron.*, **29**, 11498 (2018); https://doi.org/10.1007/s10854-018-9245-3